Title	Pion properties at finite nuclear density based on in-medium chiral perturbation theory
Author(s)	Goda, S.; Jido, D.
Citation	Progress of Theoretical and Experimental Physics (2014), 2014(3)
Issue Date	2014-03-12
URL	http://hdl.handle.net/2433/188882
Right	© The Author(s) 2014. Published by Oxford University Press on behalf of the Physical Society of Japan.; This is an Open Access article distributed under the terms of the Creative Commons Attribution License (http://creativecommons.org/licenses/by/3.0/), which permits unrestricted reuse, distribution, and reproduction in any medium, provided the original work is properly cited.
Type	Journal Article
Textversion	publisher

PTEP

Prog. Theor. Exp. Phys. **2014**, 033D03 (26 pages)
DOI: 10.1093/ptep/ptu023

Pion properties at finite nuclear density based on in-medium chiral perturbation theory

Soichiro Goda[1,*] and Daisuke Jido[2]

[1]*Department of Physics, Graduate School of Science, Kyoto University Kyoto 606-8502, Japan*
[2]*Department of Physics, Tokyo Metropolitan University, Hachioji, Tokyo 192-0397, Japan*
*E-mail: gouda@ruby.scphys.kyoto-u.ac.jp

Received December 03, 2013; Accepted January 22, 2014; Published March 11, 2014

The in-medium pion properties, i.e. the temporal pion decay constant f_t, the pion mass m_π^*, and the wave function renormalization in symmetric nuclear matter are calculated in an in-medium chiral perturbation theory up to the next-to-leading order of the density expansion $O(k_F^4)$. The chiral Lagrangian for the pion–nucleon interaction is determined in vacuum, and the low-energy constants are fixed by experimental observables. We carefully define the in-medium state of the pion and find that the pion wave function renormalization plays an essential role in the in-medium pion properties. We show that the linear density correction is dominant and the next-to-leading corrections are not so large at the saturation density, while their contributions can be significant at higher densities. The main contribution of the next-to-leading order comes from the double scattering term. We also discuss whether the low-energy theorems, the Gell-Mann–Oakes–Renner relation and the Glashow–Weinberg relation, are satisfied in the nuclear medium beyond the linear density approximation. We also find that the wave function renormalization is enhanced as much as 50% at the saturation density including the next-to-leading contribution, and that the wave function renormalization can be measured in the in-medium $\pi^0 \to \gamma\gamma$ decay.

Subject Index D33

1. Introduction

Spontaneous breakdown of chiral symmetry (χSSB) $SU(N_f)_L \times SU(N_f)_R \to SU(N_f)_V$ characterizes the vacuum and low-energy dynamics of quantum chromodynamics (QCD) [1,2]. The non-vanishing chiral condensate $\langle \bar{q}q \rangle$ is considered as one of the order parameters of χSSB and gives a characteristic scale for hadron physics. χSSB is considered to be responsible for the origin of the constituent quark mass after the current quark mass is partly given by the Higgs condensate. According to the spontaneous breakdown, pseudoscalar mesons such as π, K, η appear as Nambu–Goldstone (NG) bosons.

Recently, in order to investigate the mechanism of dynamical mass generation, partial restoration of the chiral symmetry in the nuclear medium has gained considerable attention. This phenomenon is the incomplete restoration of chiral symmetry with sufficient reduction of the absolute value of the chiral condensate in the medium and will lead to various changes of hadron properties. Once we understand the partial restoration of chiral symmetry, we can predict other in-medium hadronic quantities through low-energy theorems and vice versa.

From this point of view, vast theoretical and experimental efforts are devoted to this topic. The density dependence of the chiral condensate is evaluated in various approaches, e.g., the well

known linear density approximation providing the model-independent low-density theorem [3,4], the relativistic Bruckner–Hartree–Fock theory approach [5], and systematic calculations by in-medium chiral perturbation theory beyond the linear density calculation [6,7]. According to the model-independent linear density approximation, the leading density correction to the chiral condensate is determined by the πN sigma term $\sigma_{\pi N}$ and, with the empirical value of the sigma term, it has been found that the leading correction gives a large enough contribution at the normal nuclear density:

$$\frac{\langle\bar{q}q\rangle^*}{\langle\bar{q}q\rangle_0} \approx 1 - 0.35\rho/\rho_0, \tag{1}$$

where $\langle\bar{q}q\rangle^*$, $\langle\bar{q}q\rangle_0$ are the in-medium and in-vacuum condensates and ρ_0 is the normal nuclear density. Recently, an in-medium sum rule satisfied in any density region has been derived model-independently by the current algebra method and the low-energy theorems, such as the Gell-Mann–Oakes–Renner relation, the Glashow–Weinberg relation, and the Weinberg–Tomozawa relation, are discussed within the linear density order [8].

To investigate the pion properties in nuclei, deeply bound pionic atoms have received much attention [9–11]. Theoretically, the binding energies and decay widths of the 1s and 2p deeply bound pionic atom states are estimated [12–14] and in Refs. [15,16] hadronic quantities, such as the pion optical potential, have been calculated beyond the linear density. Experimentally, the reduction of the chiral condensate is estimated quantitatively through reduction of the s-wave isovector parameter b_1 in the π–nucleus optical potential [11]. The b_1 parameter is regarded as an in-medium isovector πN scattering length. These results show that the reduction of b_1 means the repulsive enhancement of the s-wave π–nucleon interaction in the nucleus. Other examples are low-energy π–nucleus scattering and $\pi\pi$ interaction in nuclei in the scalar–isoscalar channel. The low-energy π–nucleus scattering also show that s-wave π–nucleus interaction are enhanced repulsively [17,18]. According to the theoretical discussion given in Refs. [19,20], the in-medium $\pi\pi$ interaction in the scalar–isoscalar part also has attractive enhancement thanks to the partial restoration of chiral symmetry in the nuclear medium; the experimental observation of the invariant mass spectrum of the $\pi\pi$ production off nuclear targets performed in Refs. [21–23] could have a hint of such a enhancement.

In particular, the pion decay constant is a fundamental quantity of chiral symmetry breaking. The in-medium decay constant has also been investigated in the linear density approximation [24] and recently the chiral condensate and the decay constant have been evaluated in the next-to-leading order based on chiral order counting [25]. In this paper, we discuss a general in-medium pion state and evaluate in-medium pionic quantities such as the decay constant, mass, and the pseudoscalar coupling beyond the linear density approximation. This paper is organized as follows. In Sect. 2, we explain the general formulation of the in-medium chiral perturbation theory and discuss an expansion by Fermi momentum counting. In Sect. 3, we discuss the in-medium pion state and define the in-medium pionic quantities. Here we will find that the pion wave function renormalization plays an important role in the in-medium pionic quantities. In Sect. 4, we evaluate the in-medium pion self-energy, wave function renormalization, pion decay constant, and pseudoscalar coupling and show the numerical results of their density dependence up to $O(k_F^4)$ in the Fermi momentum expansion in symmetric nuclear matter and in the isospin limit. We also discuss whether the in-medium low-energy theorems, the Gell-Mann–Oakes–Renner relation and the Glashow–Weinberg relation, are satisfied or not. Finally we discuss the in-medium $\pi_0 \to 2\gamma$ process caused by the chiral anomaly. In Sect. 5, we summarize our paper.

2. In-medium chiral perturbation theory

Chiral perturbation theory (CHPT) is a powerful tool describing the low-energy dynamics of the Nambu–Goldstone (NG) bosons and nucleons as an effective field theory of QCD [26–29]. CHPT is constructed based on chiral symmetry and its spontaneous breaking and consists in systematic expansion of NG boson momentum and the quark mass. The chiral order counting scheme makes it possible to categorize Lagrangian and Feynman diagrams in terms of powers of momentum and the quark mass, and to estimate the magnitude of possible corrections for the amplitude, such as the current–current correlation functions. Thus, CHPT describes quantitatively the S-matrix elements of the QCD currents.

In this decade, chiral effective theory for nuclear matter has been developed [15,30] and is applied to study nuclear matter properties, such as the nuclear matter energy density [31], and also used to study partial restoration of chiral symmetry and the in-medium changes of the pion properties, such as in-medium pion mass, decay constant [7,25], and the 1s and 2p energy levels of deeply bound pionic atoms [12].

2.1. *Basics of the formulation*

For the calculations of the in-medium pion quantities, we evaluate the Green's functions in the ground state of nuclear matter; in particular, our interests are hadron properties in the nuclear medium as a bound state of the nucleon many-body system. In quantum field theory, the transition amplitude between the ground state in the presence of the external fields is the fundamental quantity, and the generating functional is defined by the transition amplitude, which can be calculated by the path integral formalism of the quantum field theory. In the in-medium chiral perturbation theory, one prepares the ground state of the nucleon Fermi gas at an asymptotic time as a reference state [30]. The generating functional W for the connected Green functions in nuclear matter is given as follows:

$$Z[J] = \exp i\,W[J] = \langle \Omega_{\rm out}|\Omega_{\rm in}\rangle_J \tag{2}$$

$$= \int DU\,DN\,DN^\dagger \langle \Omega_{\rm out}|N(+\infty)\rangle e^{i\int dx(\mathcal{L}_\pi+\mathcal{L}_{\pi N}+\mathcal{L}_N)}\langle N(-\infty)|\Omega_{\rm in}\rangle, \tag{3}$$

where U is the chiral field parametrized by the NG boson field in the nonlinear realization of chiral symmetry, N is the nucleon field, and J represents the scalar, pseudoscalar, vector, and axial vector external fields $J = (s, p, v, a)$. The Lagrangian is described by the free pion and nucleon fields and should include, in principle, all the interactions between pions and nucleons within the Lagrangian. Since we use a Lagrangian described by the free nucleon field and this Lagrangian prescribes the nucleon interaction, the reference state can be the ground state of the free Fermi gas of nucleons defined by

$$|\Omega_{\rm in,out}\rangle \equiv \prod_n^N a^\dagger(\mathbf{p}_n)|0\rangle, \tag{4}$$

where $a^\dagger(\mathbf{p}_n)$ is the nucleon creation operator with momentum $\mathbf{p}_n$, the index n represents the spin and isospin, N is the number of momentum states below the nucleon Fermi momentum $k_F^{(n)}$, which is obtained by the nucleon density ρ_n as $k_F^{(n)} = (3\pi^2\rho_n)^{1/3}$, and $|0\rangle$ is the 0-particle state.

The connected n-point Green functions can be calculated by taking functional derivatives of $i\,W[J]$ with respect to the external sources J_i:

$$\langle \Omega_{\rm out}|T\mathcal{O}_1\cdots\mathcal{O}_n|\Omega_{\rm in}\rangle = (-i)^n \frac{\delta}{\delta J_1}\cdots\frac{\delta}{\delta J_n} i\,W[J], \tag{5}$$

where $\mathcal{O}_i$ is the corresponding current operator to the external source J_i. Considering the symmetry property of the current operator under the chiral rotation, one can identify the quark contents of the current operators, such as the pseudoscalar current $P^i = \bar{q} i\gamma_5 \tau^i q$ and the axial vector current $A^i_\mu = \bar{q}\gamma_\mu\gamma_5\tau^i q/2$. If we evaluate the generating functional nonperturbatively with appropriate nucleon–nucleon interactions, we can describe the nuclear matter in principle and deduce the QCD current Green functions in nuclear matter. Note that this prescription resembles the description of the deuteron in terms of free nucleons, in which one starts with the free nucleon field and appropriate nucleon–nucleon interaction and can find the deuteron as a bound state of two nucleons by solving the Bethe–Salpeter equation nonperturbatively.

In Ref. [30], a method is proposed to derive the in-medium chiral Lagrangian in a systematic expansion in terms of the chiral counting and the Fermi sea insertion. In this method, the Fermi momentum is regarded as a small parameter of the chiral order. Performing the integral in terms of the nucleon field by using the Gauss integral formula for the bilinear form of the nucleon interaction, one obtains a generating functional characterized by double expansion of Fermi sea insertions and chiral orders:

$$Z[J] = \int DU \exp\left\{ i \int dx \left[\mathcal{L}_{\pi\pi} - \int \frac{d\mathbf{p}}{(2\pi)^3 2E_p} \mathcal{F}\,\mathrm{Tr}\Big(i\Gamma(x,y)(\not{p} + m_N) n(p) \Big) - \frac{i}{2} \int \frac{d\mathbf{p}}{(2\pi)^3 2E_p} \right.\right.$$
$$\left.\left. \frac{d\mathbf{q}}{(2\pi)^3 2E_q} \mathcal{F}\,\mathrm{Tr}\Big(i\Gamma(x,x')(\not{q} + m_N) n(q) i\Gamma(x',y)(\not{p} + m_N) n(p) \Big) + \cdots, \right] \right\} \tag{6}$$

where $\mathcal{F}$ denotes Fourier transformation of the spatial variables except for x, $E(\mathbf{p})$ is the nucleon energy $E(\mathbf{p}) = \sqrt{\mathbf{p}^2 + m_N^2}$ for the momentum $\mathbf{p}$, and $\Gamma(x, y)$ is the nonlocal vertex defined by the in-vacuum quantities as $\Gamma \equiv -iA[1_4 - G_0 A]^{-1}$, where the interactions A and the free nucleon propagator G_0 are given by the in-vacuum chiral perturbation theory. The isodoublet matrix $n(p)$ restricts the momentum integral for the nucleon momenta up to the Fermi momentum:

$$n(p) = \begin{pmatrix} \theta(k_F^p - |\mathbf{p}|) & 0 \\ 0 & \theta(k_F^n - |\mathbf{p}|) \end{pmatrix}. \tag{7}$$

The nonlocal vertex $\Gamma(x, y)$ is expanded in terms of the bilinear local vertex A as

$$i\Gamma = A + AG_0A + AG_0AG_0A + \cdots \tag{8}$$

and the vertex A is also expanded in terms of the chiral order. The in-medium pion Lagrangian $\tilde{\mathcal{L}}_{\pi\pi}$ can be obtained by the generating functional (6) as $Z[J] = \exp[i \int d^4x \tilde{\mathcal{L}}_{\pi\pi}]$.

For the calculation of the amplitude, one uses free nucleon propagators for the chiral expansion of the nonlocal vertex function and the Fermi sea nucleon term $(-2\pi)\delta(p^2 - m_N^2)\theta(p_0)n(p)$ in the Fermi sea insertion among the nonlocal vertices $\Gamma(x, y)$. It has been shown explicitly in Ref. [32] that this expansion scheme is consistent with the conventional relativistic many-body theory in the sense that one can use the in-medium nucleon propagator directly, i.e. the Fermi gas propagator,

$$iG^i(p) = iG^i_0(p) + iG^i_m(p) \tag{9}$$
$$= \frac{i(\not{p} + m_N)}{p^2 - m_N^2 + i\epsilon} - 2\pi(\not{p} + m_N)\delta(p^2 - m_N^2)\theta(p_0)\theta(k_F^i - |\mathbf{p}|), \tag{10}$$

in the calculation. Here, the free propagator and the medium part of the Fermi gas propagator are denoted by iG^i_0, iG^i_m with the isospin index $i = n, p$. The medium part iG^i_m represents the Fermi sea effect. We can calculate the connected functions using the usual perturbative expansions with the

in-medium nucleon propagator. In this way, one can deal with density contributions from the nuclear medium by perturbative expansion of the nuclear Fermi momentum.

2.2. *Density expansion*

In in-medium CHPT, we can classify the current Green functions in terms of the order of the small parameters in the expansion of the pion momentum, the quark mass, and the Fermi momentum in a similar way to in-vacuum CHPT. The chiral order of a specific diagram is counted as [30]

$$\nu = 4L_\pi - 2I_\pi + \sum_{i=1}^{V_\pi} d_i + \sum_{i=1}^{V_\rho} d_{\rho i} \geq 4 \tag{11}$$

$$d_\rho = 3n + \sum_{i=1}^{n} \nu_{\Gamma_i} - 4(n-1) \tag{12}$$

where L_π is the number of pion loops, I_π is the number of pion propagators, d_i is the chiral dimension from the pion chiral Lagrangian, d_ρ is the chiral dimension of the nonlocal in-medium vertex with n Fermi sea insertions, and ν_Γ is the chiral dimension of the Γ vertex. In this chiral counting, we count the Fermi gas propagator as $O(p^{-1})$, like a free nucleon propagator, so that the counting rule is the same as for in-vacuum chiral perturbation theory.

In this work, we focus on the Fermi momentum dependence of the Green functions and count only by Fermi momentum orders. We assume that the in-vacuum loop effects are renormalized into counter-terms in the chiral Lagrangian and we use the in-vacuum physical values to fix the low-energy constants (LECs). For example, we translate LEC c_1 appearing in $\mathcal{L}^{(2)}_{\pi N}$ into the physical πN sigma term $\sigma_{\pi N}$:

$$c_1 = -\frac{\sigma_{\pi N}}{4m_\pi^2}, \tag{13}$$

since the c_1 term gives the leading order of the πN sigma term in the chiral perturbation theory and, once one calculates the higher orders for the πN sigma term, they should also contribute to the in-medium quantities in the same manner as c_1. An empirical value for the sigma term is $\sigma_{\pi N} \simeq 45$ MeV [33], and a recent analysis based on relativistic formulation of πN chiral perturbation theory suggests $\sigma_{\pi N} = 59(7)$ MeV [34,35]. Another example is the isoscalar πN scattering length a^+. In tree order, a^+ is given with LECs c_1, c_2, c_3 from $\mathcal{L}^{(2)}_{\pi N}$ as

$$b^+ \equiv 4\pi \left(1 + \frac{m_\pi}{m_N}\right) a^+ = \frac{2m_\pi^2}{f_\pi^2} \left(2c_1 - c_2 - c_3 + \frac{g_A^2}{8m_N}\right). \tag{14}$$

The scattering length is used to determine the combination of the LECs c_1, c_2, c_3. Recent calculations based on CHPT give $a^+ = (7.6 \pm 3.1) \times 10^{-3}\, m_\pi^{-1}$ at better than 95% confidence level [36]. In this way, we take the in-vacuum physical values to determine the LECs and perform systematic calculations for density effects of the pionic observables based on the counting of Fermi momentum orders.

As we have discussed in Ref. [32], beyond the order of ρ^2 in the density expansion, the πN dynamics alone cannot predict the in-medium quantities, because we encounter divergence in loop calculations. This divergence can be removed, once we introduce counter-terms expressed by NN contact interactions. The NN interactions are to be determined by the in-vacuum NN dynamics.

2.3. *Chiral Lagrangian and parametrization of chiral field*

We use the following chiral Lagrangian in this work. The chiral Lagrangian for the meson sector is given with the chiral field U parametrized by the pion field as

$$\mathcal{L}_\pi^{(2)} = \frac{f^2}{4}\mathrm{Tr}\left(D_\mu U^\dagger D^\mu U + \chi^\dagger U + \chi U^\dagger\right), \tag{15}$$

with the covariant derivative for the chiral field U

$$D_\mu U = \partial_\mu U - i(v_\mu + a_\mu)U + iU(v_\mu - a_\mu) \tag{16}$$

given by the vector and axial vector external fields v_μ and a_μ counted as $O(p)$, and the χ field

$$\chi = 2B_0(s + ip) \tag{17}$$

given by the scalar and pseudoscalar fields s and p counted as $O(p^2)$. The scalar field s is replaced by the quark mass matrix in calculation. This Lagrangian is counted as $O(p^2)$.

In this paper, in order to simplify the perturbative calculation, as we did in our previous paper [32], we use the following parametrization of the chiral field U, proposed by [38,39]:

$$U = \exp\left[i\pi^i\tau^i\frac{y(\pi^2)}{2\sqrt{\pi^2}}\right] \tag{18}$$

where $y(\pi^2)$ satisfies

$$y - \sin y = \frac{4}{3}\left(\frac{\pi^2}{f^2}\right)^{\frac{3}{2}}. \tag{19}$$

The chiral Lagrangian for the nucleon sector is as follows:

$$\mathcal{L}_{\pi N} = \bar{N}(i\gamma^\mu\partial_\mu - m_N - A)N, \tag{20}$$

where A is the chiral interaction for the nucleon in the bilinear form. The chiral interaction can be expanded in terms of the chiral order as $A = \sum_{n=1} A^{(n)}$, and $A^{(n)}$ is counted as $O(p^n)$. The explicit form of the leading term $A^{(1)}$ reads

$$A^{(1)} = -i\gamma^\mu\Gamma_\mu - ig_A\gamma^\mu\gamma_5\Delta_\mu \tag{21}$$

with the vector current

$$\Gamma_\mu = \frac{1}{2}[u^\dagger, \partial_\mu u] - \frac{i}{2}u^\dagger(v_\mu + a_\mu)u - \frac{i}{2}u(v_\mu - a_\mu)u^\dagger, \tag{22}$$

and the axial current

$$\Delta_\mu = \frac{1}{2}\Big[u^\dagger\big(\partial_\mu - i(v_\mu + a_\mu)\big)u - u\big(\partial_\mu - i(v_\mu - a_\mu)\big)u^\dagger\Big], \tag{23}$$

where the field u is defined by a square root of the chiral field U: $u = \sqrt{U}$. The expression of the next leading term $A^{(2)}$ is given as

$$A^{(2)} = -c_1\langle\chi_+\rangle + \frac{c_2}{2m_N^2}\langle u_\mu u_\nu\rangle D^\mu D^\nu - \frac{c_3}{2}\langle u_\mu u^\mu\rangle \tag{24}$$

with $\chi_+ \equiv u\chi^\dagger u + u^\dagger\chi u^\dagger$, $u_\mu \equiv 2i\Delta_\mu$, and the covariant derivative for the nucleon field $D_\mu N = (\partial_\mu + \Gamma_\mu)N$. Here we have omitted irrelevant terms in the present work for the in-medium pion properties in symmetry nuclear matter.

3. In-medium properties of the pion

3.1. Pion mass and wave function renormalization

The in-medium pion propagation can be calculated by the two-point function of the pseudoscalar density:

$$\Pi^{ab}(p) = \langle \Omega | P^a P^b | \Omega \rangle. \tag{25}$$

Around the in-medium pion pole the two-point function can be written in terms of the in-medium quantities, such as the in-medium pion mass m_π^{*2}, velocity v_π, and pseudoscalar coupling G_π^*, as

$$\Pi^{ab}(p) = \delta^{ab} G_\pi^* \frac{i}{p_0^2 - v_\pi^2 \mathbf{p}^2 - m_\pi^{*2} + i\epsilon} G_\pi^* \tag{26}$$

where G_π^* does not include any singularity at the pion pole. In this way, with $\mathbf{p} = 0$, the in-medium pion mass is defined by the pole position of the two-point function and the coupling of the pion to the pseudoscalar density P^a in medium is defined by the square root of the residue of the two-point function at the pion pole.

The two-point function can be calculated using the in-medium chiral perturbation theory given in the previous section. The calculation will be done in terms of in-vacuum quantities like

$$\Pi^{ab}(p) = \delta^{ab} \hat{G}_\pi \frac{i}{p^2 - m_\pi^2 - \Sigma(p^2) + i\epsilon} \hat{G}_\pi, \tag{27}$$

where m_π is the in-vacuum pion mass, $\Sigma(p^2)$ is the pion self-energy in medium, and $\hat{G}_\pi$ is the vertex correction of the pion coupling to the pseudoscalar density. The vertex correction $\hat{G}_\pi$ does not contain the pion pole and it is calculated by considering one-particle irreducible diagrams.

Expanding the self-energy $\Sigma(p^2)$ in Eq. (27) around $p_0^2 = m_\pi^{*2}$ and $\mathbf{p}^2 = 0$,

$$\Sigma(p^2) = \Sigma(m_\pi^{*2}) + (p_0^2 - m_\pi^{*2}) \frac{\partial \Sigma(m_\pi^{*2})}{\partial p_0^2} + \mathbf{p}^2 \frac{\partial \Sigma(m_\pi^{*2})}{\partial \mathbf{p}^2} + \cdots,$$

we write the two-point function in the following way:

$$\Pi^{ab}(p) = \delta^{ab} \hat{G}_\pi \frac{iZ}{p_0^2 - v_\pi^2 \mathbf{p}^2 - m_\pi^{*2} + i\epsilon} \hat{G}_\pi \tag{28}$$

with

$$m_\pi^{*2} = m_\pi^2 + \Sigma(m_\pi^{*2}) \tag{29}$$

$$v_\pi^2 = 1 + \frac{\partial \Sigma(m_\pi^{*2})}{\partial \mathbf{p}^2} \tag{30}$$

$$Z = \left(1 - \frac{\partial \Sigma}{\partial p_0^2}(m_\pi^{*2}) \right)^{-1}. \tag{31}$$

Comparing Eqs. (26) and (28), we obtain, at the pion pole,

$$G_\pi^* = \sqrt{Z} \hat{G}_\pi. \tag{32}$$

Using the in-medium chiral perturbation theory we can calculate the self-energy $\Sigma(p^2)$ and $\hat{G}_\pi$; thus, we obtain the in-medium pion properties with the above equations.

3.2. *In-medium state*

The in-medium pion propagator can also be written by the pion field operator π as

$$\langle\Omega|\pi^a\pi^b|\Omega\rangle = \delta^{ab}\frac{i}{p^2 - m_\pi^2 - \Sigma(p^2) + i\epsilon} \tag{33}$$

$$= \delta^{ab}\frac{iZ}{p_0^2 - v_\pi^2\mathbf{p}^2 - m_\pi^{*2} + i\epsilon}. \tag{34}$$

Comparing Eqs. (28) and (34), for the calculation of the pion pole we regard

$$\pi^a = \frac{P^a}{\hat{G}_\pi}. \tag{35}$$

The pion operator π creates one pion in medium with mass m_π^* and wave function normalization Z, satisfying

$$\langle\Omega|\pi^a|\pi^{*b}(p)\rangle = \delta^{ab}\sqrt{Z}, \tag{36}$$

where we have introduced the one-pion state with a momentum p in the nuclear medium by denoting $|\pi^{*b}\rangle$.

The in-medium coupling constant G_π^* defined in Eq. (26) as the residue of the pion propagator induced by the pseudoscalar density may also be written as the following matrix element:

$$G_\pi^*\delta^{ab} = \langle\Omega|P^a|\pi^{*b}(p)\rangle. \tag{37}$$

Relation (32) can be understood by Eq. (37) with the reduction formula:

$$\begin{aligned}
\langle\Omega|P^a|\pi^{*b}(p)\rangle &= \lim_{p^2\to m_\pi^{*2}}\left(\frac{i\sqrt{Z}}{p^2 - m_\pi^{*2} + i\epsilon}\right)^{-1}\langle\Omega|P^a\pi^b|\Omega\rangle \\
&= \lim_{p^2\to m_\pi^{*2}}\left(\frac{i\sqrt{Z}}{p^2 - m_\pi^{*2} + i\epsilon}\right)^{-1}\frac{1}{\hat{G}_\pi}\langle\Omega|P^aP^b|\Omega\rangle \\
&= \lim_{p^2\to m_\pi^{*2}}\left(\frac{i\sqrt{Z}}{p^2 - m_\pi^{*2} + i\epsilon}\right)^{-1}\frac{1}{\hat{G}_\pi}\delta^{ab}\left(\frac{\hat{G}_\pi iZ\hat{G}_\pi}{p^2 - m_\pi^2 + i\epsilon}\right) \\
&= \delta^{ab}\sqrt{Z}\hat{G}_\pi
\end{aligned}$$

where we have understood $p^2 = p_0^2 - v_\pi^2\mathbf{p}^2$, and we have used Eq. (35) in the second equality and Eq. (28) in the third equality.

3.3. *In-medium pion decay constants*

We define the in-medium decay constant in analogy with the in-vacuum decay constant as a matrix element of the axial vector current A_μ^a:

$$\langle\Omega|A_\mu^a(0)|\pi^{*b}(p)\rangle = i\big[p_\mu F^*(p_0,\mathbf{p}) + n_\mu(p\cdot n)N^*(p_0,\mathbf{p})\big]\delta^{ab} \tag{38}$$

where we have introduced a vector characterizing the medium rest frame n_μ with $n^2 = 1$ and there are two form factors, F^* and N^*, in the presence of nuclear matter. In fact, these form factors should be functions of p^2 and $p\cdot n$, according to Lorentz covariance. The pion decay constants are obtained

at the mass shell point with $|\mathbf{p}| = 0$ and $p_0 = m_\pi^*$. We define the temporal and spatial components of the decay constant f_t, f_s by taking $n_\mu = (1, \mathbf{0})$ as

$$\langle \Omega | A_0^a | \pi^{*b} \rangle \equiv i f_t p_0, \tag{39}$$

$$\langle \Omega | A_i^a | \pi^{*b} \rangle \equiv i f_s p_i. \tag{40}$$

The decay constants are obtained by

$$f_t = F^*(m_\pi^*, \vec{0}) + N^*(m_\pi^*, \vec{0}), \tag{41}$$

$$f_s = N^*(m_\pi^*, \vec{0}). \tag{42}$$

These decay constants can be calculated in the in-medium chiral perturbation theory. Making good use of the reduction formula in momentum space again, we write down the matrix element in terms of the one-particle irreducible vertex correction and the wave function renormalization:

$$\begin{aligned}
\langle \Omega | A_\mu^a | \pi^{*b}(p) \rangle &= \lim_{p^2 \to m_\pi^{*2}} \left(\frac{i\sqrt{Z}}{p^2 - m_\pi^{*2} + i\epsilon} \right)^{-1} \langle \Omega | A_\mu^a \pi^b | \Omega \rangle \\
&= \lim_{p^2 \to m_\pi^{*2}} \left(\frac{i\sqrt{Z}}{p^2 - m_\pi^{*2} + i\epsilon} \right)^{-1} \frac{1}{\hat{G}_\pi} \langle \Omega | A_\mu^a P^b | \Omega \rangle \\
&= \lim_{p^2 \to m_\pi^{*2}} \left(\frac{i\sqrt{Z}}{p^2 - m_\pi^{*2} + i\epsilon} \right)^{-1} \frac{1}{\hat{G}_\pi} i \hat{f}_i p_\mu \left(\frac{iZ}{p^2 - m_\pi^{*2} + i\epsilon} \right) \hat{G}_\pi \\
&= i \hat{f}_i \sqrt{Z} p_\mu,
\end{aligned}$$

where we mean $p^2 = p_0^2 - v_\pi^2 \mathbf{p}^2$, and $\hat{f}_i$ with $i = t, s$ is the vertex correction of the decay constant, which can be calculated by one-particle irreducible diagrams in the chiral perturbation theory.

4. Results

In this section, we investigate explicitly the in-medium pion properties with the in-medium chiral perturbation theory up to the order of k_F^4 in the density expansion. In the last section, we found that the in-medium pion decay constant can be calculated by the pion wave function renormalization Z and the one-particle irreducible vertex correction $\hat{f}_i$. The wave function renormalization is evaluated by taking the derivative of the pion self-energy Σ with respect to the energy squared. We calculate the pion self-energy first. With the self-energy, we then evaluate the in-medium pion mass and the wave function renormalization, and show their density dependence. Calculating the one-particle irreducible correction for the pion decay constant, we evaluate the density dependence of the decay constant with the wave function renormalization. We also check whether the low-energy relations are also satisfied in the nuclear medium. Finally we discuss the $\pi^0 \to 2\gamma$ decay rate in the nuclear medium. For simplicity, we concentrate on the calculation under the unpolarized symmetric nuclear matter, where the matter has spin 0 and isospin 0 with equal proton and neutron densities, $\rho_p = \rho_n$.

In the following, we present the Feynman diagrams for each quantity and classify them according to the density dependence. As we have already discussed in the previous section, we presume that the in-vacuum LECs are fixed by the experimental observables. The vertex and mass corrections from the quantum loops of the pion and the nucleon are renormalized into physical quantities. On this understanding, we replace the LECs with the observed quantities and use the experimental values.

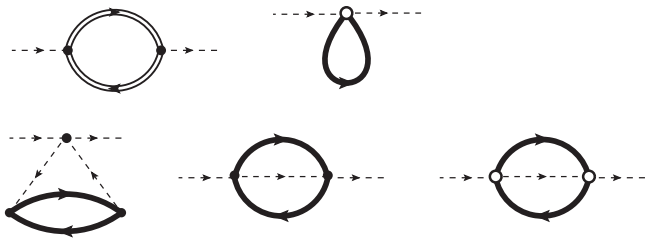

Fig. 1. Feynman diagrams for the pion self-energy Σ up to $O(k_F^4)$. (a) The leading order of the density corrections $O(k_F^3)$. (b) The next-to-leading order correction $O(k_F^4)$. In these diagrams, the dashed lines denote the pion lines, the doubled and thick lines are the nucleon lines for the Fermi gas propagator iG and the medium part of the Fermi gas propagator iG_m, and the filled and unfilled circles are the leading and the next-to-leading order vertices from the chiral Lagrangian, respectively.

In the present work the relevant replacements are as follows:

$$2B_0 m_q \to m_\pi^2 \tag{43}$$

$$c_1 \to -\frac{\sigma_{\pi N}}{4m_\pi^2} \tag{44}$$

$$2c_1 - c_2 - c_3 \to \frac{f_\pi^2}{2m_\pi^2} b^+ - \frac{g_A^2}{8m_N} \tag{45}$$

where the left-hand sides are given by LECs, while the right-hand sides are written in terms of the observed quantities in vacuum. In these expressions, $b^+ \equiv 4\pi(1 + m_\pi/m_N)a^+$ with the isoscalar πN scattering length a^+. In the replacement, higher-order contributions in the chiral counting are already involved. In this sense, we lose the strict counting of the chiral order. Taking this scheme, we do not have to calculate the loop integrals that contain only the in-vacuum propagators, because they are supposed to be already counted inside the experimental value. This fact reduces the number of relevant diagrams that we should calculate.

The in-medium quantities that we are going to calculate should be evaluated at the pion pole. The in-vacuum chiral order can be counted by the pion mass. Therefore, in the perturbative expansion, the term of which the leading chiral counting in vacuum is ℓ has $m_\pi^\ell k_F^m (\frac{k_F}{m_N})^n$ dependence. The factor $(k_F/m_N)^n$ comes from the Fermi motion correction of the nucleon when one calculates the Fermi sea loop integral. The order of the density expansion is counted as $p = m + n$, while the order of the small parameter is given by $q = \ell + m$. If one takes the density contribution up to $k_F^4 \sim \rho^{4/3}$, it is sufficient to consider diagrams with $q \leq m + 4$.

The details of the loop calculation are summarized in Appendix A.

4.1. In-medium pion self-energy

We show the Feynman diagrams contributing the in-medium self-energy with the density corrections up to $O(k_F^4 \sim \rho^{4/3})$ in Fig. 1. In these diagrams, the dashed, doubled, and thick lines are the pion propagator, the Fermi gas propagator iG, and the nucleon propagation in the Fermi gas iG_m, and the filled and unfilled circles are the leading and next-to-leading order vertices from the chiral Lagrangian, respectively. In the following calculations, we fix the external momentum as $q = (q_0, \mathbf{0})$.

The diagrams for the leading order of the density expansion $O(k_F^3)$ are given in Fig. 1(a). The self-energy coming from the left-hand diagram Σ_1 in Fig. 1 (a) can be calculated as

$$\begin{aligned} -i\Sigma_1(q_0) &= -\int \frac{d^4p}{(2\pi)^4}\mathrm{Tr}\Big[(-iA_\pi^{(1)})iG(p+q)(-iA_\pi^{(1)})iG(p)\Big] \\ &= -\rho\frac{ig_A^2}{4f^2m_N}q_0^2, \end{aligned} \tag{46}$$

where $iG(p)$ is the Fermi gas propagator given in Eq. (10), and the amplitude $-iA_\pi^{(1)}$ can be obtained by the interaction Lagrangian given in Eq. (A7) of Appendix A.

Next, we calculate the right-hand diagram Σ_2 in Fig. 1(a):

$$\begin{aligned} -i\Sigma_2(q_0) &= (-1)\int \frac{d^4p}{(2\pi)^4}\mathrm{Tr}\Big[(-iA_{\pi\pi}^{(2)})iG_m(p)\Big] \\ &= -\frac{2i\rho}{f^2}\Big(4c_1B_0m_q - (c_2+c_3)q_0^2\Big). \end{aligned} \tag{47}$$

The next-to-leading order contribution coming from the left-hand diagram Σ_3 in Fig. 1(b) is given as

$$-i\Sigma_3(q_0) = \frac{1}{2}\int \frac{d^4k}{(2\pi)^4} i\mathcal{L}_{\pi^4}^{(2)}(iD_\pi(k))^2(-i\Sigma_m(k)) \tag{48}$$

with the pion propagator $iD_\pi(k)$, the symmetric factor $1/2$, and $\Sigma_m(k)$ defined as

$$-i\Sigma_m(k) = -\int \frac{d^4p}{(2\pi)^4}\mathrm{Tr}\Big[(-iA_\pi^{(1)})iG_m(p+k)(-iA_\pi^{(1)})iG_m(p)\Big].$$

Finally we obtain

$$-i\Sigma_3(q_0) = \frac{im_\pi^2 g_A^2 k_F^4}{12\pi^4 f^4} F\left(\frac{m_\pi^2}{4k_F^2}\right) \tag{49}$$

with function $F(x^2)$ defined by

$$F(x^2) = \frac{3}{8} - \frac{3x^2}{4} - \frac{3x}{2}\arctan\frac{1}{x} + \frac{3x^2}{4}(x^2+2)\ln\frac{x^2+1}{x^2} \tag{50}$$

The self-energies coming from the double scattering corrections [37] given by the middle and right-hand diagrams of Fig. 1(b), Σ_4 and Σ_5, have two $\pi\pi NN$ vertices from the leading Weinberg–Tomozawa interaction and the next-to-leading interaction with LECs c_i, respectively. These are evaluated as

$$\begin{aligned} -i\Sigma_4(q_0) &= -\int \frac{d^4p}{(2\pi)^4}\frac{d^4k}{(2\pi)^4}\mathrm{Tr}\left[(-iA_{\pi\pi}^{(1)})iG_m\left(k-\frac{p}{2}\right)\left(-iA_{\pi\pi}^{(1)}\right)iG_m\left(k+\frac{p}{2}\right)iD_\pi(p+q)\right] \\ &= -\frac{2iq_0^2}{f^4}\frac{k_F^4}{6\pi^4}G(a^2), \end{aligned} \tag{51}$$

$$\begin{aligned} -i\Sigma_5(q_0) &= -\int \frac{d^4p}{(2\pi)^4}\frac{d^4k}{(2\pi)^4}\mathrm{Tr}\left[(-iA_{\pi\pi}^{(2)})iG_m\left(k-\frac{p}{2}\right)(-iA_{\pi\pi}^{(2)})iG_m\left(k+\frac{p}{2}\right)iD_\pi(q-p)\right] \\ &= -i\Big(8c_1B_0m_q - 2c_2q_0^2 - 2c_3q_0^2\Big)^2\frac{2k_F^4}{3\pi^4f^4}G(a^2) \end{aligned} \tag{52}$$

with $a^2 = (q_0^2 - m_\pi^2)/(4k_F^2)$ and function $G(a^2)$ defined by

$$G(x^2) = \frac{3}{8} + \frac{x^2}{4} + \frac{\sqrt{x^2}}{2}\ln\left|\frac{1-x}{1+x}\right| + \frac{x^2}{4}(x^2-3)\ln\left|\frac{1-x^2}{x^2}\right|. \tag{53}$$

Summing up all the contributions, we obtain the the self-energy up to $O(k_F^4)$ as

$$\Sigma(q_0, \mathbf{0}) = \Sigma_1 + \Sigma_2 + \Sigma_3 + \Sigma_4 + \Sigma_5 \tag{54}$$

$$= \frac{2\rho}{f^2}\left(4c_1 B_0 m_q - \left(c_2 + c_3 - \frac{g_A^2}{8m_N}\right)q_0^2\right) - \frac{m_\pi^2 g_A^2 k_F^4}{12\pi^4 f^4} F\left(\frac{m_\pi}{2k_F}\right)$$

$$+ \left[\frac{q_0^2}{8} + \left(4c_1 B_0 m_q - c_2 q_0^2 - c_3 q_0^2\right)^2\right]\frac{8k_F^4}{3f^4\pi^4} G(a^2) \tag{55}$$

with $a^2 = (q_0^2 - m_\pi^2)/(4k_F^2)$.

4.2. *In-medium pion mass*

The in-medium pion mass is obtained by the summation of the in-vacuum mass and the self-energy evaluated at the pion on the mass shell $q^\mu = (m_\pi^*, \mathbf{0})$. This brings us to a self-consistent equation:

$$m_\pi^{*2} \equiv m_\pi^2 + \Sigma(q_0^2 = m_\pi^{*2}). \tag{56}$$

Nevertheless, because the in-medium correction starts with the linear density $\rho \sim k_F^3$ and we are evaluating the pion mass up to $O(\rho^{4/3})$, the density correction on the mass in the argument of the self-energy gives higher orders in the density expansion of the in-medium pion mass. Thus, we are allowed to evaluate the self-energy at the in-vacuum on-shell $q^\mu = (m_\pi, \mathbf{0})$ for the present purpose. We evaluate the in-medium pion mass up to $O(\rho^{4/3})$ as

$$m_\pi = \sqrt{m_\pi^2 + \Sigma(q_0^2 = m_\pi^2)}$$

$$= m_\pi\left\{1 + \frac{\rho}{f^2}\left(2c_1 - c_2 - c_3 + \frac{g_A^2}{8m_N}\right) - \frac{g_A^2 k_F^4}{24\pi^4 f^4} F\left(\frac{m_\pi}{2k_F}\right)\right.$$

$$\left. + \left[\frac{1}{8} + m_\pi^2\left(2c_1 - c_2 - c_3\right)^2\right]\frac{4k_F^4}{3\pi^4 f^4} G(0)\right\}$$

$$= m_\pi\left\{1 + \rho\frac{b^+}{2m_\pi^2} - \frac{g_A^2 k_F^4}{24\pi^4 f_\pi^4} F\left(\frac{m_\pi}{2k_F}\right) + \left[\frac{1}{8} + m_\pi^2\left(\frac{b^+}{2m_\pi^2} - \frac{g_A^2}{8m_N}\right)^2\right]\frac{2k_F^4}{\pi^4 f_\pi^4}\right\}. \tag{57}$$

The LECs, B_0, c_1, c_2, c_3, have been determined by the in-vacuum physical quantities, the pion mass m_π, the πN sigma term $\sigma_{\pi N}$, and the factored scattering length b^+. The linear density correction of the pion mass stems from the scattering length. Since the isosinglet πN scattering length is known to be small compared to the inverse pion mass, $b^+ = (9.6 \pm 3.9) \times 10^{-2}\, m_\pi^{-1}$, the leading correction is as small as 5% at the saturation density $\rho_0 \simeq 0.49\, m_\pi^3$.

In Fig. 2, we show the density dependence of the in-medium pion mass as a function of the density normalized by the normal nuclear density ρ_0. In the figure, the dotted line shows the result up to the leading linear density and the solid line is for the result containing the next-to-leading order. We take the following values for the in-vacuum quantities: $f_\pi = 92.4\,\text{MeV}$, $g_A = 1.26$, $m_\pi = 138\,\text{MeV}$, $b^+ = 9.6 \times 10^{-2}\, m_\pi^{-1}$, and $\sigma_{\pi N} = 45\,\text{MeV}$ [33]. One can see from Fig. 2 that the next-to-leading order (NLO) correction is not small. The main contribution comes from the double scattering terms. The density correction of the pion mass at twice or three times the normal nuclear density becomes about 15 to 20%. Since the in-medium CHPT is a low-energy effective theory it would be not applicable in the higher-density region; nevertheless, we expect that this theory would be applicable up to $3\rho_0$ where Fermi momentum corresponds to about 400 MeV.

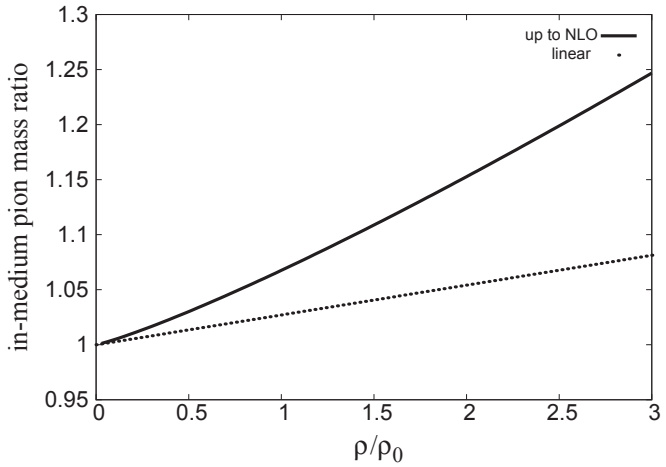

Fig. 2. Density dependence of the in-medium pion mass normalized by the in-vacuum pion mass, m_π^*/m_π, in symmetric nuclear matter. The dotted line shows the result up to the leading linear density correction, while the solid line is the result containing the next-to-leading order correction.

4.3. In-medium wave function renormalization

Next, the wave function renormalization is obtained by evaluating the derivative of the self-energy $\Sigma(q_0)$ with respect to q_0^2 at $q_0^2 = m_\pi^{*2}$. Again, since the difference between the in-medium and in-vacuum pion masses in the self-energy is counted as the higher order of the density expansion, we evaluate the derivative of the self-energy at $q_0^2 = m_\pi^2$ for the present purpose:

$$\begin{aligned} Z &= \left[1 - \frac{\partial \Sigma(q_0^2 = m_\pi^2)}{\partial q_0^2}\right]^{-1} \\ &= \left[1 + \frac{2\rho}{f^2}\left(c_2 + c_3 - \frac{g_A^2}{8m_N}\right) - \left(\frac{1}{8m_\pi^2} - 2(2c_1 - c_2 - c_3)(c_2 + c_3)\right)\frac{8m_\pi^2 k_F^4}{3\pi^4 f^4} G(0)\right]^{-1} \\ &= 1 + \frac{2\rho}{f_\pi^2}\left(\frac{\sigma_{\pi N}}{2m_\pi^2} + \frac{f_\pi^2 b^+}{2m_\pi^2}\right) \\ &\quad + \frac{m_\pi^2 k_F^4}{\pi^4 f_\pi^4}\left[\frac{1}{8m_\pi^2} + 2\left(\frac{f_\pi^2 b^+}{2m_\pi^2} - \frac{g_A^2}{8m_N}\right)\left(\frac{\sigma_{\pi N}}{2m_\pi^2} + \frac{f_\pi^2 b^+}{2m_\pi^2} - \frac{g_A^2}{8m_N}\right)\right]. \end{aligned} \tag{58}$$

In the calculation of the wave function renormalization, we encounter a singularity in the derivative of function $G(x)$ at $x \to 0$. As discussed in detail in Appendix A, this singularity may be considered as an infrared singularity in quantum field theory and brings a problematic density dependence starting from $k_F^2 \ln k_F$, which is inconsistent with the low-density expansion starting from k_F^3. Thus, we should expect certain cancellation of the singularity. The infrared singularity should cancel when one calculates the scattering rates, not in the amplitude itself. Therefore we have dropped the singular term containing the derivative of function $G(x)$.

At the linear density, we find that

$$Z = 1 + 0.40\frac{\rho}{\rho_0}, \tag{59}$$

which implies that the wave function is enhanced by 40% at the saturation density. The density dependence of the wave function renormalization is shown in Fig. 3. As one can see in the figure, the density correction of the wave function is not so small, being of the order of 50% at the saturation

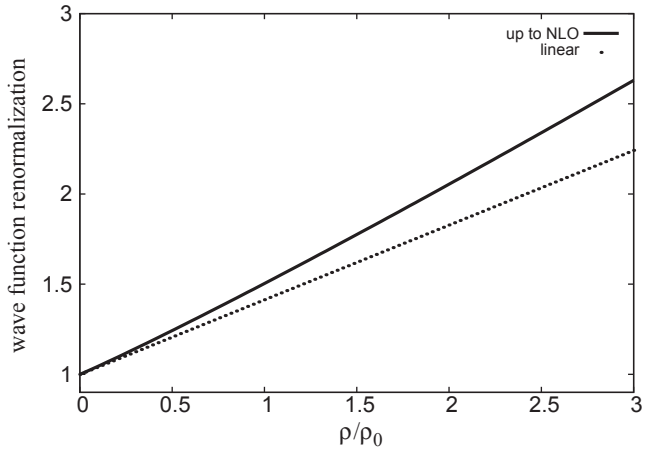

Fig. 3. Density dependence of the in-medium pion wave function renormalization Z in symmetric nuclear matter. The dotted line shows the result up to the leading linear density correction and the solid line is for the pion mass containing the next-to-leading order correction.

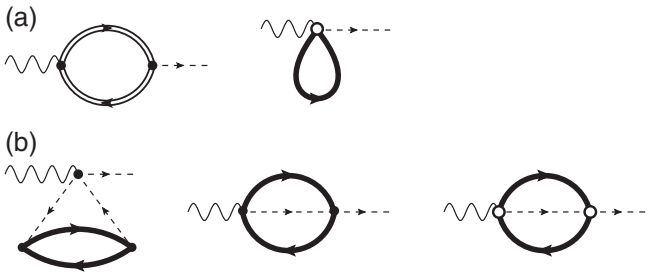

Fig. 4. Feynman diagrams showing the one-particle vertex correction of the pion decay constant $\hat{f}_t$. (a) Leading order density corrections. (b) Next-to-leading order corrections. In these diagrams, the wavy line denotes the axial vector current.

density. It would be very interesting if one could observe the strong enhancement of the wave function renormalization phenomenologically, such as in formation cross sections of deeply bound pionic atoms. Later, we will again discuss the possible observation of the wave function renormalization itself in the in-medium π^0 decay into 2γ.

4.4. In-medium pion decay constant

We evaluate the temporal pion decay constant in medium. According to the discussion in the previous section, the in-medium decay constant is given by the wave function renormalization Z and the one-particle irreducible vertex correction $\hat{f}_t$ as $f_t = \hat{f}_t\sqrt{Z}$. The wave function renormalization has already been evaluated in the previous subsection; here let us calculate the vertex correction $\hat{f}_t$ in density expansion.

In Fig. 4, we show the relevant Feynman diagrams for the density corrections up to $O(k_F^4 \sim \rho^{4/3})$. The wavy lines in Fig. 4 denote axial vector currents. The leading graphs $O(k_F^3)$ are shown in Fig. 4(a), while the next-to-leading order contributions $O(k_F^4)$ are given in Fig. 4(b). Since the temporal decay constant is given by the matrix element of the time component of the axial vector current A_0^i, we evaluate the one-particle irreducible (1PI) matrix element

$$\langle\Omega|A_0^i|\pi^{*j}(q)\rangle_{\rm 1PI} = i\delta^{ij}\, p_0 \hat{f}_t \tag{60}$$

for the rest pion $q_\mu = (q_0, \mathbf{0})$. The loop calculation is essentially the same as the calculation done for the self-energy. Here we will show only the definition and result of each contribution.

The contribution from the left-hand diagram $\hat{f}_1$ in Fig. 4(a) reads

$$\hat{f}_1 q_0 = -\int \frac{d^4p}{(2\pi)^4} \mathrm{Tr}\Big[(-iA_a^{(1)}) iG(p+q)(-iA_\pi^{(1)}) iG(p)\Big] = -q_0 \frac{g_A^2}{4fm_N}\rho. \tag{61}$$

The vertex correction coming from the right-hand diagram in Fig. 4(a) is

$$\hat{f}_2 q_0 = -\int \frac{d^4p}{(2\pi)^4} \mathrm{Tr}\Big[(-iA_{\pi a}^{(2)}) iG_m(p)\Big] = q_0 \frac{2\rho}{f}(c_2+c_3). \tag{62}$$

For the left-hand diagram in Fig. 4(b), we have $\hat{f}_3$ with symmetric factor 1/2:

$$\begin{aligned}\hat{f}_3 q_0 &= \frac{1}{2}\int \frac{d^4k}{(2\pi)^4} i\mathcal{L}_{\pi^3 a}^{(2)} \big(iD_\pi(k)\big)^2 (-i\Sigma_m) \\ &= q_0 \frac{g_A^2 k_F^4}{6\pi^4 f^3} F\left(\frac{m_\pi^2}{4k_F^2}\right).\end{aligned} \tag{63}$$

Function $F(x)$ is defined in Eq. (50). The vertex corrections represented by the middle and right-hand diagrams in Fig. 4(b) are calculated as

$$\begin{aligned}\hat{f}_4 q_0 &= -\int \frac{d^4p}{(2\pi)^4}\frac{d^4k}{(2\pi)^4} \mathrm{Tr}\left[(-iA_{\pi a}^{(1)}) iG_m\left(k-\frac{p}{2}\right)(-iA_{\pi\pi}^{(1)}) iG_m\left(k+\frac{p}{2}\right) iD_\pi(p+q)\right] \\ &= -\frac{q_0 k_F^4}{3\pi^4 f^4} G(a^2)\end{aligned} \tag{64}$$

$$\begin{aligned}\hat{f}_5 q_0 &= -\int \frac{d^4p}{(2\pi)^4}\frac{d^4k}{(2\pi)^4} \mathrm{Tr}\left[(-iA_{\pi a}^{(2)}) iG_m\left(k-\frac{p}{2}\right)(-iA_{\pi\pi}^{(2)}) iG_m\left(k+\frac{p}{2}\right) iD_\pi(q-p)\right] \\ &= (c_2+c_3)\Big(2c_1 m_\pi^2 - (c_2+c_3)q_0^2\Big)\frac{8q_0 k_F^4}{3\pi^4 f^3} G\left(a^2\right)\end{aligned} \tag{65}$$

where $a^2 = (q_0^2 - m_\pi^2)/(4k_F^2)$ and function $G(x)$ is defined in Eq. (53).

The vertex correction $\hat{f}_t$ should be evaluated at $q_0^2 = m_\pi^{*2}$ in principle, because the decay constant is the matrix element of the axial current of the in-medium pion state having the on-shell condition $q_0 = m_\pi^*$. However, in practice, we are allowed to evaluate the vertex correction at $q_0 = m_\pi$, because the difference is in the higher-density orders.

Summing up all the contributions, we obtain the density dependence of $\hat{f}_t$ up to $O(k_F^4)$:

$$\hat{f}_t(q_0 = m_\pi) = \hat{f}_1 + \hat{f}_2 + \hat{f}_3 + \hat{f}_4 + \hat{f}_5 \tag{66}$$

$$\begin{aligned}&= f + \frac{2\rho}{f}\left(c_2 + c_3 - \frac{g_A^2}{8m_N}\right) + \frac{g_A^2 k_F^4}{6\pi^4 f^3} F\left(\frac{m_\pi}{2k_F}\right) \\ &\quad - \left[\frac{1}{8} - (c_2+c_3)(2c_1 - c_2 - c_3)\right]\frac{8m_\pi^2 k_F^4}{3\pi^4 f^3} G(0) \\ &= f_\pi\Big[1 - \frac{2\rho}{f_\pi^2}\Big(\frac{\sigma_{\pi N}}{2m_\pi^2} + \frac{f_\pi^2 b^+}{2m_\pi^2}\Big) + \frac{g_A^2 k_F^4}{6\pi^4 f_\pi^4} F\left(\frac{m_\pi}{2k_F}\right) \\ &\quad - \frac{m_\pi^2 k_F^4}{\pi^4 f_\pi^4}\left[\frac{1}{8} + \left(\frac{f_\pi^2 b^+}{2m_\pi^2} - \frac{g_A^2}{8m_N}\right)\left(\frac{\sigma_{\pi N}}{2m_\pi^2} + \frac{f_\pi^2 b^+}{2m_\pi^2} - \frac{g_A^2}{8m_N}\right)\right]\end{aligned} \tag{67}$$

where we have used $G(0) = 3/8$.

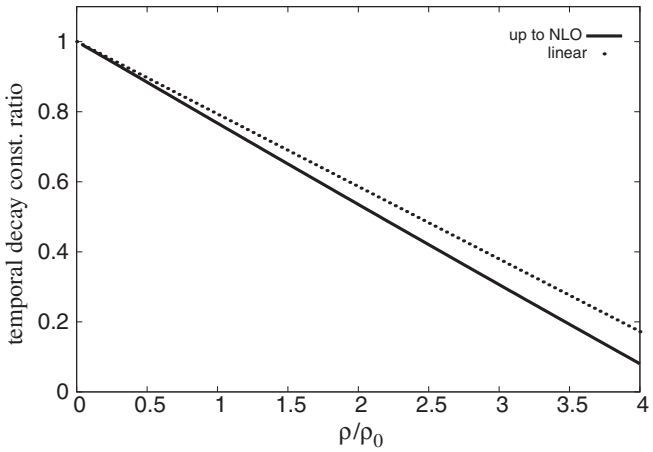

Fig. 5. Density dependence of the temporal decay constant normalized by the in-vacuum pion decay constant f_π in symmetric nuclear matter. The dotted line is for the result in the leading linear density and the solid line is for the result including the next-to-leading order.

With $\hat{f}_t$, we can calculate the in-medium pion decay constant:

$$\begin{aligned} f_t &= \hat{f}\sqrt{Z} \\ &= f_\pi \left[1 - \frac{\rho}{f_\pi^2} \left(\frac{\sigma_{\pi N}}{2m_\pi^2} + \frac{f_\pi^2 b^+}{2m_\pi^2} \right) + \frac{g_A^2 k_F^4}{6\pi^4 f_\pi^4} F\left(\frac{m_\pi}{2k_F} \right) - \frac{k_F^4}{16\pi^4 f_\pi^4} \right]. \end{aligned} \tag{68}$$

The LECs are determined by the πN sigma term $\sigma_{\pi N}$ and the isoscalar πN scattering length b^+.

We show in Fig. 5 the density dependence of the temporal decay constant. In this figure, the dotted line is for the result of the leading linear density and the solid line is for the result including the next-to-leading order $O(k_F^4)$. We find that the NLO correction produces a change of a few percent in the low-density region but, in the high-density region, an NLO correction about three times the normal nuclear density contributes 10 percent and is not small.

Let us make some comments on the perturbative expansion in terms of the Fermi momentum. In the in-medium CHPT, the expansion parameter is to be $k_F/(4\pi f_\pi)$ and it amounts to around 0.3 to 0.4, even at a higher-density region than the saturation density. With this small value, we could say that the perturbative expansion in terms of the Fermi momentum may have good convergence. Nevertheless, if one wants to judge whether the Fermi momentum expansion is good or not in nuclear matter, one should describe the nuclear matter and reproduce the saturation properties first, and see the higher-density effects. The nuclear matter cannot be described essentially in the perturbation theory of in-vacuum fields. One would need a nonperturbative treatment to obtain the nuclear matter. In such a case, naive perturbative expansion in terms of the Fermi momentum would break down before the nuclear density.

4.5. In-medium pseudoscalar coupling

The pseudoscalar coupling G_π^* is also calculated as

$$G_\pi^* \equiv \langle \Omega | P^a | \pi^{*b} \rangle = \hat{G}_\pi \sqrt{Z}. \tag{69}$$

In Fig. 6, we show the Feynman graphs that contribute to the one-particle irreducible vertex correction $\hat{G}_\pi$. Performing the same calculation as for the pion decay constant $\hat{f}_t$, we obtain the density

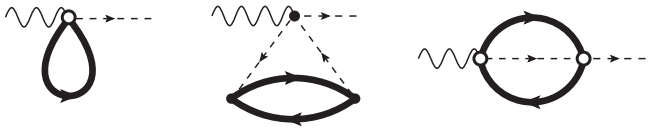

Fig. 6. Feynman diagrams contributing to the one-particle irreducible vertex correction for the pseudoscalar coupling $\hat{G}_\pi$. The wavy line is the pseudoscalar density. The left-hand diagram is the leading order density contribution, while the middle and right-hand diagrams contribute to the next-to-leading order correction.

dependence of the in-medium pseudoscalar coupling:

$$\frac{G_\pi^*}{G_\pi} = 1 + \frac{\rho}{f^2}\left(4c_1 - c_2 - c_3 + \frac{g_A^2}{8m_N}\right) + \frac{g_A^2 k_F^4}{12 f^4 \pi^4} F\left(\frac{k_F}{2m_\pi}\right) + \frac{k_F^4}{f^4\pi^4}\left(\frac{1}{16} + m_\pi^2 (2c_1 - c_2 - c_3)^2\right). \tag{70}$$

4.6. In-medium low-energy theorems

It is known that the Gell-Mann–Oakes–Renner (GOR) relation is satisfied in medium up to the linear density (see, e.g., Ref. [8]). Having obtained the density dependences of the pion decay constant and the pion mass in medium up to $O(k_F^4)$, we are going to examine the GOR relation satisfied at $O(k_F^4)$. The density dependence of the quark condensate is obtained in Ref. [32] up to $O(k_F^4)$. Using the expressions for the in-medium quantities, we obtain

$$\frac{f_t^2}{f_\pi^2}\frac{m_\pi^{*2}}{m_\pi^2} - \frac{\langle \bar{u}u + \bar{d}d\rangle^*}{\langle \bar{u}u + \bar{d}d\rangle_0} = \frac{8m_\pi^2 k_F^4}{3\pi^4 f^4}\left[(2c_1 - c_2 - c_3)^2 G(0) - 4c_1^2 G_1\left(\frac{m_\pi^2}{4k_F^2}\right)\right] \tag{71}$$

$$G_1(x^2) = G(-x^2) = \frac{3}{8} - \frac{x^2}{4} - x \arctan\frac{1}{x} + \frac{x^2}{4}(x^2+3)\ln\left|\frac{1+x^2}{x^2}\right|. \tag{72}$$

From this equation, we find that the GOR relation is not satisfied at this order and the double scattering terms break the relation. The reason for the breaking is as follows: The GOR relation connects the chiral condensate and the pion quantities. The chiral condensate is calculated in the soft limit by taking $q \to 0$ in the correlation function, while the pionic quantities are evaluated for the pion on the mass shell. Off the chiral limit, where the pion is massive, the two energy points are different. This difference causes the GOR relation to break.

In the chiral limit in vacuum, one has the Glashow–Weinberg (GW) relation $f_\pi G_\pi = -\langle \bar{q}q\rangle$. This relation is known to be satisfied in medium in the chiral limit and at the linear density [8]. Here we also directly check whether the relation is satisfied in the order $O(k_F^4)$ off the chiral limit:

$$\frac{f_t^*}{f_\pi}\frac{G_\pi^*}{G_\pi} - \frac{\langle \bar{u}u + \bar{d}d\rangle^*}{\langle \bar{u}u + \bar{d}d\rangle_0} = \frac{8m_\pi^2 k_F^4}{3\pi^4 f^4}\left[(2c_1 - c_2 - c_3)^2 G(0) - 4c_1^2 G_1\left(\frac{m_\pi^2}{4k_F^2}\right)\right]. \tag{73}$$

As seen in this equation, the GW relation is broken by the double scattering term and the breaking terms correspond to the right-hand side in Eq. (72).

It is also interesting to discuss the in-medium sum rule for the in-medium quark condensate derived in Ref. [8] model-independently in the chiral limit:

$$-\langle \bar{q}q\rangle = \mathrm{Re}\sum_\alpha f_\alpha G_\alpha, \tag{74}$$

where α is the label of the zero-modes in nuclear matter, such as pions and particle–hole excitations, and the summation is taken over all of the zero modes. It has been shown that, in the linear density, only the pion zero mode can contribute to the sum rule and one obtains the in-medium Glashow–Weinberg relation $f_t G_\pi^* = -\langle \bar{q}q \rangle^*$. The other zero modes, such as particle–hole excitations, contribute only as higher-density corrections. As discussed in Ref. [32], the NN correlation effects come into the chiral effective theory from the order of $O(\rho^2)$. Thus, we expect that the pion mode dominates the sum rule beyond the linear density but below the square density order in the chiral limit. We can check this by taking the chiral limit in Eq. (73). This means that the GW relation is satisfied up to $O(k_F^4)$ in the chiral limit:

$$f_t G_\pi^* = -\langle \bar{u}u + \bar{d}d \rangle. \tag{75}$$

With this relation, realizing that both f_t and G_π^* decrease as the density increases, we find that the chiral condensate decreases more rapidly than the pion decay constant. Although one might have some corrections from $O(\rho^2)$ contributions, this observation could be a hint that at a certain higher density the chiral condensate would become zero before the pion decay constant was zero. In this situation, even though the quark condensate is zero, the chiral symmetry is spontaneously broken.

4.7. *In-medium π^0 decay to 2γ*

The neutral π^0 meson decays dominantly into 2γ in vacuum through the quantum effect known as the axial anomaly. Here let us estimate the medium modification of the decay rate of π^0 to 2γ by following the formulation presented in Sect. 3. The decay amplitude may be written, as required by Lorentz invariance, in the form

$$\langle \pi^{0*} | \gamma\gamma \rangle = -i M_{\gamma\gamma}^* \epsilon^{\mu\nu\alpha\beta} \epsilon_\mu^* k_\nu \epsilon_\alpha'^* k'_\beta, \tag{76}$$

where $M_{\gamma\gamma}^*$ stands for the decay amplitude in medium, $\epsilon^{\mu\nu\alpha\beta}$ is the totally antisymmetric tensor, ϵ_μ^* and $\epsilon_\alpha^{*\prime}$ are the polarization vectors of the emitted photons, and k_ν and k'_β are the momenta of the photon. According to the argument given in Sect. 3, the in-medium amplitude $M_{\gamma\gamma}^*$ can be written as

$$M_{\gamma\gamma}^* = \sqrt{Z} \hat{M}_{\gamma\gamma} \tag{77}$$

with the wave function renormalization Z and the medium correction of the one-particle irreducible $\pi^0\gamma\gamma$ vertex $\hat{M}_{\gamma\gamma}$.

In the nuclear medium, the π^0 meson may decay into 2γ through non-anomalous diagrams because of the presence of nucleons, which can bring out the intrinsic parity violated in the $\pi^0 \to 2\gamma$ process. Nevertheless, in Ref. [7], it was found that there are no medium corrections to the $\pi^0 \to 2\gamma$ amplitude up to $\mathcal{O}(p^5)$, i.e., the linear density correction in the density expansion. The argument is based on the spin and flavor structure of the vertices. The nucleon 1-loop with the $\pi^0\gamma\gamma NN$ contact vertex should vanish because the contact vertex contains γ_5 and there are no other vertices that can bring γ_5 into the nucleon loop, which makes the trace of the Dirac matrices vanish. The diagrams in which the photons and the neutral pion emit sequentially from a nucleon also turn out to vanish according to careful calculation of the flavor matrix. Hence, the in-medium correction up to the linear density vanishes and the in-medium vertex correction $\hat{M}_{\gamma\gamma}$ amplitude is equivalent to the in-vacuum amplitude $M_{\gamma\gamma}$. This leads to the conclusion that the in-medium correction of the decay amplitude

$M^*_{\gamma\gamma}$ can be calculated solely by the wave function renormalization as

$$\frac{M^*_{\gamma\gamma}}{M_{\gamma\gamma}} = \sqrt{Z}. \tag{78}$$

Ignoring the small density correction of the pion mass in the phase space of the decay process, we find that the modification of the π^0 decay rate to 2γ in nuclear matter is given by the wave function renormalization as

$$\frac{\Gamma^*}{\Gamma_0} = Z. \tag{79}$$

This implies that the π^0 decay into 2γ in nuclear matter measures directly the in-medium renormalization of the π^0 wave function in lower density. Using the result discussed in the previous subsections, we obtain the linear density approximation as

$$\frac{\Gamma^*}{\Gamma_0} = 1 + 0.4\frac{\rho}{\rho_0}. \tag{80}$$

At normal nuclear density the decay rate is enhanced 1.4 times and the partial width becomes about 10 eV.

5. Summary

We have discussed in-medium pion properties, such as the pion decay constant, the pion mass, and the wave function renormalization based on the in-medium chiral perturbation theory. First, we have provided a general formalism of the in-medium chiral perturbation theory and have discussed an expansion in terms of Fermi momentum. Assuming that the renormalization for the in-vacuum quantities is performed in an appropriate way, we use the observed values to determine the low-energy constants (LECs) in the chiral Lagrangian. Since we have used the physical values, the higher-order corrections for the momentum expansion are implicitly included in the calculation. Thus, we focus on the expansion of the Fermi momentum of the physical quantities, which are calculated by the QCD current Green functions. To calculate the in-medium quantities, we carefully define the in-medium pion state, and we have found that the in-medium wave function renormalization plays an essential role in defining the in-medium coupling constants, such as the decay constant and pseudoscalar coupling constant.

We have evaluated the density dependence of the decay constant, the pion mass, the pion wave function renormalization, and the pseudoscalar coupling including the next-to-leading order of the density expansion beyond the well known linear density approximation based on the in-medium chiral perturbation theory. We have found that the $O(k_F^4)$ corrections cause a change of a few percent in the low-density region for the decay constant and the pion mass, while at higher densities, such as three times saturation density, the corrections can be of the order of 10 to 20 percent and can make a significant contribution. We have also found that the wave function renormalization is enhanced by as much as 50 percent at the saturation density. The main contribution among the corrections comes from the double scattering term. In addition, we have checked whether the low-energy theorems, the Gell-Mann–Oakes–Renner relation and the Glashow–Weinberg relation, are satisfied in medium beyond the linear density approximation. We have found that these relations are not satisfied at $O(k_F^4)$ off the chiral limit. The origin of this breaking is that we use different energy values to evaluate the pion quantities and the chiral condensate; we take the soft limit to obtain the chiral condensate, while we take the pion on the shell point, i.e. $q_0 = m^*_\pi$, to evaluate the pion quantities. Finally, we have discussed the density dependence of the $\pi^0 \to \gamma\gamma$ decay width. Considering the spinor and flavor

vertex structure of the chiral interactions, we have found that the density dependence of the π^0 width comes from the wave function renormalization alone at linear density order. With this observation, the wave function renormalization Z would be measured directly in the decay process.

Acknowledgements

This work was partially supported by Grants-in-Aid for Scientific Research (No. 25400254, No. 24105706, and No. 24540274).

Appendix A. Explicit expression for each interaction term

In order to simplify the perturbative calculation, we use the following parametrization of pion field U given by Refs. [38,39], as we did in our previous paper [32]:

$$U = \exp\left[i\pi^i\tau^i\frac{y(\pi^2)}{2\sqrt{\pi^2}}\right] \tag{A1}$$

where $y(\pi^2)$ satisfies

$$y - \sin y = \frac{4}{3}\left(\frac{\pi^2}{f^2}\right)^{\frac{3}{2}}. \tag{A2}$$

The expansion of the chiral field U in terms of the pion field is given in Ref. [38] as

$$U = 1 + \frac{i\pi^i\tau^i}{f} - \frac{\pi^2}{2f^2} - \frac{i\pi^i\tau^i\pi^2}{10f^3} - \frac{(\pi^2)^2}{40f^4} + \cdots \tag{A3}$$

and for the chiral field u

$$u = 1 + \frac{i\pi^i\tau^i}{2f} - \frac{\pi^2}{8f^2} + \frac{i\pi^i\tau^i\pi^2}{80f^3} - \frac{9(\pi^2)^2}{640f^4} + \cdots. \tag{A4}$$

In this parametrization, the soft pion theorems, such as Adler's condition, remain satisfied in simple perturbation theory. In addition, we show chiral interactions that we use in the following calculation.

With this parametrization, one finds the explicit expression for each interaction term in the chiral Lagrangian. The chiral interactions for pions are as follows:

$$\mathcal{L}^{(2)}_{\pi^4} = -\frac{1}{10f^2}\partial_\mu\pi^i\partial^\mu\pi^j\pi^k\pi^l(\delta^{ij}\delta^{kl} - 3\delta^{ik}\delta^{jl}) - \frac{m_q B_0}{20f^2}\pi^i\pi^j\pi^k\pi^l\delta^{ij}\delta^{kl}, \tag{A5}$$

$$\mathcal{L}^{(2)}_{\pi^3 a} = \frac{1}{5f}a^i_\mu\partial^\mu\pi^j\pi^k\pi^l(3\delta^{ij}\delta^{kl} - 4\delta^{ik}\delta^{jl}). \tag{A6}$$

The interactions containing the nucleon in the bilinear form read

$$A^{(1)}_\pi = \frac{g_A}{2f}\gamma^\mu\gamma_5\partial_\mu\phi^i\tau^i \tag{A7}$$

$$A^{(1)}_a = -g_A\gamma^\mu\gamma_5 a^i_\mu\frac{\tau^i}{2} \tag{A8}$$

$$A^{(1)}_{\pi a} = \frac{i}{2f}\gamma^\mu[\phi, a_\mu] = -\frac{1}{2f}\gamma^\mu\phi^i a^j_\mu\epsilon^{ijk}\tau^k \tag{A9}$$

$$A^{(2)}_{\pi a} = -\frac{2c_2}{fm_N^2}\partial_\mu\phi^i a^i_\nu\partial^\mu\partial^\nu + \frac{2c_3}{f}\partial_\mu\phi^i a^{\mu i}. \tag{A10}$$

Appendix B. Details of self-energy calculations

In this appendix, we show the details of the self-energy calculations shown in Sect. 4. We consider the isospin symmetric limit and the symmetric nuclear matter. The external momentum is fixed as $q = (q_0, \mathbf{0})$ for simplicity. We write the nucleon propagator in the Fermi sea as

$$iG_m(p) = -2\pi(\not{p} + m_N)\delta(p^2 - m_N^2)\theta(p_0)\theta(k_F - |\mathbf{p}|). \tag{B1}$$

For the Pauli-blocked nucleon propagator in the symmetric nuclear matter $iG(p)$, we use the following expression, which is equivalent to Eq. (10):

$$iG(p) = i\frac{\not{p} + m_N}{2E(\mathbf{p})}\left(\frac{1-\theta(k_F-|\mathbf{p}|)}{p_0 - E(\mathbf{p}) + i\epsilon} + \frac{\theta(k_F-|\mathbf{p}|)}{p_0 - E(\mathbf{p}) - i\epsilon} + \frac{1}{p_0 + E(\mathbf{p}) - i\epsilon}\right) \tag{B2}$$

$$= i\frac{\not{p} + m_N}{2E(\mathbf{p})}G_r(p). \tag{B3}$$

We also define the propagator $iG_r(p)$ in which the spinor structure and the nucleon energy are factored out from $iG(p)$. In the following calculation, the trace symbol Tr implies taking the trace in both the spinor and isospin spaces, while Tr_s means the trace for only the spinor space.

1-loop integrals

We first calculate the pion self-energy given by the diagram on the left of Fig. 1(a):

$$\begin{aligned}
-i\Sigma_1(q_0)\delta^{ij} &= -\int\frac{d^4p}{(2\pi)^4}\mathrm{Tr}\Big[(-iA_\pi^{(1)})iG(p+q)(-iA_\pi^{(1)})iG(p)\Big] \\
&= -\int\frac{d^4p}{(2\pi)^4}\mathrm{Tr}\left[(-i)\frac{g_A}{2f}\gamma_5 i\ \not{q}\tau^i i\frac{\not{p}+\not{q}+m_N}{2E(\mathbf{p}+\mathbf{q})}G_r(p+q)\right. \\
&\quad\left.\times\ (-i)\frac{g_A}{2f}(-\gamma_5)i\ \not{q}\tau^j i\frac{\not{p}+m_N}{2E(\mathbf{p})}G_r(p)\right] \\
&= -\delta^{ij}\frac{g_A^2}{2f^2}\int\frac{d^4p}{(2\pi)^4}\mathrm{Tr}_s\Big[\ \not{q}(\not{p}+\not{q}-m_N)\ \not{q}(\not{p}+m_N)\Big]\frac{G_r(p+q)G_r(p)}{2E(\mathbf{p})2E(\mathbf{p}+\mathbf{q})}.
\end{aligned} \tag{B4}$$

The spinor trace can be calculated as

$$f_{\mathrm{Tr}}(p_0) = \mathrm{Tr}_s\left[\not{q}(\not{p}+\not{q}-m_N)\ \not{q}(\not{p}+m_N)\right] = 4(p\cdot q)\{(p+q)^2 - p^2\} - 4q^2(p^2+m_N^2).$$

For the calculation of the integral, we perform the p_0 integral first using the Cauchy theorem along a contour of the upper semicircle in the complex p_0-plane:

$$\begin{aligned}
&\int\frac{dp^0}{2\pi}f_{\mathrm{Tr}}(p_0)G_r(p+q)G_r(p) \\
&= 2i\left[f_{\mathrm{Tr}}(E(\mathbf{p})-q_0)\frac{(E(\mathbf{p})-q_0)\theta(k_F-|\mathbf{p}|)}{q_0(q_0-2E(\mathbf{p}))} + f_{\mathrm{Tr}}(E(\mathbf{p}))\frac{(E(\mathbf{p})+q_0)\theta(k_F-|\mathbf{p}|)}{q_0(q_0+2E(\mathbf{p}))}\right] \\
&= 8iq_0^2 m_N\theta(k_F-|\mathbf{p}|).
\end{aligned}$$

Here we have picked up only the terms including the step function, because the vacuum part should be subtracted for the calculation of the in-medium quantities, and in the final expression we have taken the leading term in the $1/m_N$ expansion.

Finally we obtain

$$-i\Sigma_1(q_0)\delta^{ij} = -\delta^{ij}\frac{ig_A^2q_0^2}{f^2m_N}\int\frac{d^3p}{(2\pi)^3}\theta(k_F-|\mathbf{p}|) = -\frac{ig_A^2q_0^2}{4f^2m_N}\delta^{ij}\rho, \tag{B5}$$

where we have used $\rho = 2k_F^3/(3\pi^2)$.

Next we consider the self-energy given by the right-hand diagram in Fig. 1(a):

$$\begin{aligned}-i\Sigma_2(q_0) &= (-1)\int \frac{d^4p}{(2\pi)^4}\mathrm{Tr}\Big[(-iA^{(2)}_{\pi\pi})iG_m(p)\Big]\\ &= \int \frac{d^3p}{(2\pi)^3}(-4i)\left(\frac{8B_0c_1m_q}{f^2} - \frac{2c_2}{f^2m_N^2}(q\cdot p)^2 - \frac{2c_3}{f^2}q^2\right)\theta(k_F-|\mathbf{p}|)\\ &= -\frac{2i\rho}{f^2}(4c_1B_0m_q - (c_2+c_3)q_0^2). \end{aligned} \tag{B6}$$

Here we have taken the leading term of the $1/m_N$ expansion.

2-loop integrals

Next we calculate the next-to-leading contributions in the density expansion. Here we denote the pion propagator as $iD_\pi(p)$.

First we consider the left-hand diagram in Fig. 1(b), $\Sigma_3(q_0)$: With symmetric factor $1/2$, the contribution is written as

$$-i\Sigma_3(q_0) = \frac{1}{2}\int \frac{d^4k}{(2\pi)^4} i\mathcal{L}^{(2)}_{\pi^4}(iD_\pi(k))^2(-i\Sigma_m(k)), \tag{B7}$$

where $\Sigma_m(k)$ is defined as

$$-i\Sigma_m(k) = -\int \frac{d^4p}{(2\pi)^4}\mathrm{Tr}\Big[(-iA^{(1)}_\pi)iG_m(p+k)(-iA^{(1)}_\pi)iG_m(p)\Big].$$

Using the on-shell conditions $(p+k)^2 = m_N^2$, $p^2 = m_N^2$ for the nucleon propagators in the Fermi sea, the spinor trace is calculated as follows:

$$\mathrm{Tr}_s\Big[\not{k}(\not{p}+\not{k}-m_N)\not{k}(\not{p}+m_N)\Big] = -8m_N^2k^2.$$

Hence, we obtain $\Sigma(q_0)$:

$$\begin{aligned}-i\Sigma_3(q_0) &= \frac{ig_A^2m_\pi^2}{2f^4}\int \frac{d^3k}{(2\pi)^3}\frac{d^3p}{(2\pi)^3}(iD_\pi(k))^2k^2\theta(k_f-|\mathbf{p}+\mathbf{k}|)\theta(k_f-\mathbf{p})\\ &= \frac{ig_A^2m_\pi^2}{2f^4}\int \frac{d^3k}{(2\pi)^3}\frac{d^3p}{(2\pi)^3}\frac{\mathbf{k}^2}{(\mathbf{k}^2+m_\pi^2)^2}\theta(k_f-|\mathbf{p}+\mathbf{k}|)\theta(k_f-\mathbf{p})\\ &= \frac{ig_A^2m_\pi^2k_F^4}{12\pi^4f^4}F\left(\frac{m_\pi^2}{4k_F^2}\right), \end{aligned} \tag{B8}$$

where we have used the following integral formula:

$$\int \frac{d^3k}{(2\pi)^3}\frac{d^3p}{(2\pi)^3}\frac{\mathbf{k}^2}{(\mathbf{k}^2+m_\pi^2)^2}\theta\left(k_F-\left|\mathbf{p}+\frac{\mathbf{k}}{2}\right|\right)\theta\left(k_F-\left|\mathbf{p}-\frac{\mathbf{k}}{2}\right|\right) = \frac{k_F^4}{6\pi^4}F\left(\frac{m_\pi^2}{4k_F^2}\right),$$

with function $F(a^2)$:

$$\begin{aligned}F(a^2) &= \int_0^1 dx\left(\frac{x^2}{x^2+a^2}\right)^2\frac{1}{2}(1-x)^2(x+2)\\ &= \frac{3}{8} - \frac{3a^2}{4} - \frac{3a}{2}\arctan\frac{1}{a} + \frac{3a^2}{4}(a^2+2)\ln\frac{a^2+1}{a^2}. \end{aligned}$$

We consider the contribution coming from the middle diagram in Fig. 1(b), $\Sigma_4(q_0)$:

$$
\begin{aligned}
&-i\Sigma_4(q_0)\\
&\quad=-\int\frac{d^4p}{(2\pi)^4}\frac{d^4k}{(2\pi)^4}\mathrm{Tr}\left[(-iA^{(1)}_{\pi\pi})iG_m\left(k-\frac{p}{2}\right)(-iA^{(1)}_{\pi\pi})iG_m\left(k+\frac{p}{2}\right)iD_\pi(q-p)\right]\\
&\quad=-\int\frac{d^4p}{(2\pi)^4}\frac{d^4k}{(2\pi)^4}\mathrm{Tr}\left[\frac{\epsilon^{ikm}\tau^m}{4f^2}(2\not{q}-\not{p})iG_m\left(k-\frac{p}{2}\right)\frac{\epsilon^{kjm}\tau^m}{4f^2}(2\not{q}-\not{p})iG_m\left(k+\frac{p}{2}\right)\right].
\end{aligned}
$$

Performing the integration in terms of p_0 and k_0, we obtain

$$k_0=\frac{1}{2}(E(\mathbf{k}+\mathbf{p}/2)+E(\mathbf{k}-\mathbf{p}/2)) \tag{B9}$$

$$p_0=E(\mathbf{k}+\mathbf{p}/2)-E(\mathbf{k}-\mathbf{p}/2), \tag{B10}$$

which also provide $k\cdot p=0$, $k^2+p^2/4=m_N^2$. With these expressions, the spinor trace is calculated as

$$\mathrm{Tr}_s\left[(2\not{q}-\not{p})\left(\not{k}-\frac{\not{p}}{2}+m_N\right)(2\not{q}-\not{p})\left(\not{k}+\frac{\not{p}}{2}+m_N\right)\right]=32(q\cdot k)^2-8(q\cdot p)^2+8q^2p^2.$$

In the leading term of the $1/m_N$ expansion, we have the relation $k_0=m_N$, $p_0=0$ and we obtain

$$-i\Sigma_4(q_0)=-\int\frac{d^3p}{(2\pi)^3}\frac{d^3k}{(2\pi)^3}\frac{2q_0^2}{f^4}\theta\left(k_f-\left|\mathbf{k}-\frac{\mathbf{p}}{2}\right|\right)\theta\left(k_f-\left|\mathbf{k}+\frac{\mathbf{p}}{2}\right|\right)\frac{i}{\mathbf{p}^2-(q_0^2-m_\pi^2)}.$$

Using the following integral formula [40]:

$$\int\frac{d^3k}{(2\pi)^3}\theta\left(k_f-\left|\mathbf{k}-\frac{\mathbf{p}}{2}\right|\right)\theta\left(k_f-\left|\mathbf{k}+\frac{\mathbf{p}}{2}\right|\right)=\frac{k_F^3}{6\pi^2}\left(1-\frac{3}{2}x+\frac{1}{2}x^3\right)\theta(1-x),$$

with $x=|\mathbf{p}|/(2k_F)$, we get

$$-i\Sigma_4(q_0)=-\frac{iq_0^2k_F^4}{3\pi^4f^4}G\left(\frac{q_0^2-m_\pi^2}{4k_F^2}\right), \tag{B11}$$

where we have used

$$G(a^2)=\int_0^1\frac{x^2}{x^2-a^2}(1-x)^2(x+2)dx=\frac{3}{8}+\frac{a^2}{4}+\frac{a}{2}\ln\left|\frac{1-a}{1+a}\right|+\frac{a^2}{4}(a^2-3)\ln\left|\frac{1-a^2}{a^2}\right|.$$

Finally we consider $\Sigma_5(q_0)$, given by the right-hand diagram in Fig. 1(b). This graph corresponds to the double scattering correction called the Ericson–Ericson term [37] and is calculated as:

$$
\begin{aligned}
-i\Sigma_5(q_0)&=-\int\frac{d^4p}{(2\pi)^4}\frac{d^4k}{(2\pi)^4}\mathrm{Tr}\left[(-iA^{(2)}_{\pi\pi})iG_m\left(k-\frac{p}{2}\right)(-iA^{(2)}_{\pi\pi})iG_m\left(k+\frac{p}{2}\right)iD_\pi(p+q)\right]\\
&=\int\frac{d^3p}{(2\pi)^3}\frac{d^3k}{(2\pi)^3}\mathrm{Tr}_s\left[\left(\not{k}-\frac{\not{p}}{2}+m_N\right)\left(\not{k}+\frac{\not{p}}{2}+m_N\right)\right]\frac{\delta^{ij}}{2m_N^2}iD_\pi(p+q)\\
&\quad\times\left(\frac{8c_1B_0m_q}{f^2}-\frac{2c_2}{f^2m_N^2}\left\{q\cdot\left(k-\frac{p}{2}\right)\right\}\left\{(p+q)\cdot\left(k-\frac{p}{2}\right)-\frac{2c_3}{f^2}q\cdot(p+q)\right\}\right)\\
&\quad\times\left(\frac{8c_1B_0m_q}{f^2}-\frac{2c_2}{f^2m_N^2}\left\{q\cdot\left(k+\frac{p}{2}\right)\right\}\left\{(p+q)\cdot\left(k+\frac{p}{2}\right)-\frac{2c_3}{f^2}q\cdot(p+q)\right\}\right)\\
&\quad\times\theta\left(k_f-\left|\mathbf{k}-\frac{\mathbf{p}}{2}\right|\right)\theta\left(k_f-\left|\mathbf{k}+\frac{\mathbf{p}}{2}\right|\right).
\end{aligned}
$$

The spinor trace is reduced to

$$\mathrm{Tr}_s\left[\left(\not{k}-\frac{\not{p}}{2}+m_N\right)\left(\not{k}+\frac{\not{p}}{2}+m_N\right)\right]=4k^2-p^2+m_N^2=8m_N^2-2p^2.$$

Finally $\Sigma_5(q_0)$ is obtained as

$$\begin{aligned}-i\,\Sigma_5(q_0)&=-\frac{4i}{f^4}\left(8c_1B_0m_q-2c_2q_0^2-2c_3q_0^2\right)^2\int\frac{d^3p}{(2\pi)^3}\frac{d^3k}{(2\pi)^3}\\&\quad\times\theta\left(k_f-\left|\mathbf{k}-\frac{\mathbf{p}}{2}\right|\right)\theta\left(k_f-\left|\mathbf{k}+\frac{\mathbf{p}}{2}\right|\right)\frac{1}{\mathbf{p}^2-(q^2-m_\pi^2)-i\epsilon}\\&=-\frac{4i}{f^4}\left(8c_1B_0m_q-2c_2q_0^2-2c_3q_0^2\right)^2\frac{k_F^4}{6\pi^4}G\left(\frac{q^2-m_\pi^2}{4k_F^2}\right).\end{aligned}\tag{B12}$$

In the last equality, we have performed the integral in the same way as for Σ_4.

Appendix C. Singularity in the derivative of the double scattering term

The loop integral of the double scattering term reads

$$I_{\mathrm{ds}}(q_0)=\int\frac{d^3p}{(2\pi)^3}\frac{1}{q_0^2-m_\pi^2-\mathbf{p}^2+i\epsilon}\int\frac{d^3k}{(2\pi)^3}\theta\left(k_f-\left|\mathbf{k}-\frac{\mathbf{p}}{2}\right|\right)\theta\left(k_f-\left|\mathbf{k}+\frac{\mathbf{p}}{2}\right|\right)$$

where q_0 is the energy of the external line and we have taken $\mathbf{q}=0$ for the external momentum. Performing the following integral:

$$\int\frac{d^3k}{(2\pi)^3}\theta\left(k_f-\left|\mathbf{k}-\frac{\mathbf{p}}{2}\right|\right)\theta\left(k_f-\left|\mathbf{k}+\frac{\mathbf{p}}{2}\right|\right)=\frac{k_F^4}{6\pi^2}\left(1-\frac{3}{2}x+\frac{1}{2}x^3\right)\theta(1-x),\tag{C1}$$

where $x=|\mathbf{p}|/(2k_F)$, we write the loop integral $I_{\mathrm{ds}}(k_0)$ as

$$I_{\mathrm{ds}}(q_0)=-\frac{k_F^4}{6\pi^4}\int_0^1 dx\left(1-\frac{3}{2}x+\frac{1}{2}x^3\right)\frac{x^2}{x^2-a-i\epsilon}\tag{C2}$$

where we have defined $a\equiv(q_0^2-m_\pi^2)/(4k_F^2)$. The integral with respect to x can be done straightforwardly and we obtain

$$I_{\mathrm{ds}}(q_0)=-\frac{k_F^4}{6\pi^4}\left[\frac{3}{8}+\frac{a}{4}+\frac{\sqrt{a}}{2}\ln\left|\frac{1-\sqrt{a}}{1+\sqrt{a}}\right|+\frac{a}{4}(a-3)\ln\left|\frac{1-a}{a}\right|\right].\tag{C3}$$

This function is finite in the limit of $k_0\to m_\pi$, i.e. $a\to 0$.

But the derivative of $I_{\mathrm{ds}}(q_0)$ with respect to q_0^2 has a singularity at $a\to 0$. The derivative is obtained as

$$\frac{\partial I_{\mathrm{ds}}(q_0)}{\partial q_0^2}=-\frac{k_F^2}{24\pi^4}\frac{1}{4}\left[-\frac{2}{1+\sqrt{a}}+\frac{1}{2\sqrt{a}}\ln\left|\frac{1-\sqrt{a}}{1+\sqrt{a}}\right|+(2a-3)\ln\left|\frac{1-a}{a}\right|\right].\tag{C4}$$

This function is logarithmically divergent at $a\to 0$. In addition, this loop integral starts from $k_F^2\ln k_F$ in the expansion of small k_F. This behavior contradicts the low-density expansion where the leading order should be $\rho\sim k_F^3$. Consequently, the wave function renormalization could have such a strange

density dependence, and thus this contribution is pathologic. We do not take the exact limit of $q_0 \to m_\pi$ in the evaluation. Nevertheless, we have to deal with the singularity, because the wave function renormalization would have an inconsistent density dependence with the low-density expansion and we may make an evaluation of the physical quantities very close to the singular point, where the results are numerically unreliable.

The origin of the singularity seen in the derivative of the loop function at $q_0 = m_\pi$ can be identified when one performs the derivative of Eq. (C2) in terms of q_0 and takes $a = 0$:

$$I_{\rm ds}(m_\pi) = -\frac{k_F^2}{14\pi^4}\int_0^1 dx \left(1 - \frac{3}{2}x + \frac{1}{2}x^3\right)\frac{x^2}{(x^2 - i\epsilon)^2}.$$

The integral becomes divergent when the integrand takes $x = 0$ at the end point of the integral. This singularity is very similar to the infrared divergence in quantum field theory. Such infrared divergence should be canceled with other diagrams emitting soft pions, when one calculates the scattering rates, not in the amplitude itself. Thus, the singularity found in the derivative of the loop function should be canceled with other terms, when one calculates the cross sections. Relying on the above argument, we simply drop the term that includes the infrared singularity in this work.

References

[1] Y. Nambu and G. Jona-Lasinio, Phys. Rev. **122**, 345 (1961).
[2] Y. Nambu and G. Jona-Lasinio, Phys. Rev. **124**, 246 (1961).
[3] T. D. Cohen, R. J. Furnstahl, and D. K. Griegel, Phys. Rev. C **45**, 1881 (1992).
[4] E. G. Drukarev and E. M. Levin, Prog. Part. Nucl. Phys. **27**, 77 (1991).
[5] R. Brockmann and W. Weise, Phys. Lett. B **367**, 40 (1996).
[6] N. Kaiser, P. de Homont, and W. Weise, Phys. Rev. C **77**, 025204 (2008).
[7] U. G. Meissner, J. A. Oller, and A. Wirzba, Ann. Phys. (N.Y.) **297**, 27 (2002).
[8] D. Jido, T. Hatsuda, and T. Kunihiro, Phys. Lett. B **670**, 109 (2008).
[9] K. Itahashi et al., Phys. Rev. C **62**, 025202 (2000).
[10] H. Geissel et al., Phys. Rev. Lett. **88**, 122301 (2001).
[11] K. Suzuki et al., Phys. Rev. Lett. **92**, 072302 (2004).
[12] E. E. Kolomeitsev, N. Kaiser, and W. Weise, Phys. Rev. Lett. **90**, 092501 (2003).
[13] N. Ikeno et al., Prog. Theor. Phys. **126**, 483 (2011).
[14] N. Ikeno, H. Nagahiro, and S. Hirenzaki, Eur. Phys. J. A **47**, 161 (2011).
[15] L. Girlanda, A. Rusetsky, and W. Weise, Ann. Phys. (N.Y.) **312**, 92 (2004).
[16] M. Doring and E. Oset, Phys. Rev. C **77**, 024602 (2008).
[17] E. Friedman et al., Phys. Rev. Lett. **93**, 122302 (2004).
[18] E. Friedman et al., Phys. Rev. C **72**, 034609 (2005).
[19] T. Hatsuda, T. Kunihiro, and H. Shimizu, Phys. Rev. Lett. **82**, 2840 (1999).
[20] D. Jido, T. Hatsuda, and T. Kunihiro, Phys. Rev. D **63**, 011901 (2001).
[21] F. Bonutti et al. (CHAOS Collaboration), Phys. Rev. Lett. **77** (1996).
[22] F. Bonutti et al. (CHAOS Collaboration), Nucl. Phys. A **677**, 213 (2000).
[23] P. Camerini et al. (CHAOS Collaboration), Nucl. Phys. A **735**, 89 (2004).
[24] V. Thorsson and A. Wirzba, Nucl. Phys. A **589** 633 (1995).
[25] A. Lacour, J. A. Oller, and U.-G. Meissner. J. Phys. G **37**, 125002 (2010).
[26] S. Weinberg, Physica A **96**, 327 (1979).
[27] J. Gasser and H. Leutwyler, Ann. Phys. (N.Y.) **158**, 142 (1984).
[28] J. Gasser and H. Leutwyler, Nucl. Phys. B **250**, 465 (1985).
[29] J. Gasser, M. E. Sainio, and A. Svarc, Nucl. Phys. B **307**, 779 (1988).
[30] J. A. Oller, Phys. Rev. C **65**, 025204 (2002).
[31] N. Kaiser, S. Fritsch, and W. Weise, Nucl. Phys. A **697**, 255 (2002).
[32] S. Goda and D. Jido, arXiv:1308.2660.
[33] J. Gasser, H. Leutwyler, and M. E. Sainio, Phys. Lett. B **253**, 252 (1991).
[34] J. M. Alarcon, J. M. Camalich, and J. A. Oller, Phys. Rev. D **85**, 051503 (2012).

[35] J. M. Alarcon, L. S. Geng, J. M. Camalich, and J. A. Oller, arXiv:1209.2870 [hep-ph].
[36] V. Baru et al., Phys. Lett. B **694**, 473 (2011).
[37] M. Ericson and T. E. O. Ericson, Ann. Phys. (N.Y.) **36**, 323 (1966).
[38] J. M. Charap, Phys. Rev. D **3**, 1998 (1971).
[39] I. S. Gerstein, R. Jackiw, S. Weinberg, and B. W. Lee, Phys. Rev. D **3**, 2486 (1971).
[40] A. L. Fetter and J. D. Walecka, *Quantum Theory of Many-Particle Systems* (Dover, New York, 2003).